

# Vertical movements of frost mounds in sub-Arctic permafrost regions analyzed using geodetic survey and satellite interferometry

I.Beck<sup>1,5</sup>, R. Ludwig<sup>2</sup>, M. Bernier<sup>3</sup>, T. Strozzi<sup>4</sup> and J. Boike<sup>1</sup>

[1]{Alfred Wegener Institute, Helmholtz Centre for Polar and Marine Research, Potsdam, Germany}

[2] {Department of Geography, Ludwig-Maximilians University, Munich, Germany}

[3] {Centre Eau, Terre & Environnement, Institut national de la recherche scientifique, Québec Canada}

[4]{GAMMA Remote Sensing Research and Consulting AG, Gümmlingen, Switzerland}

[5]{ GIScience Research Group, Institute of Geography, Heidelberg University}

Correspondence to: I. Beck (inga.beck@awi.de)

## Abstract

Permafrost-affected soils cover about ~~450~~ – ~~45~~ % of Canada. The environment in such areas, especially those located within the discontinuous permafrost zone, has been impacted more than any other by recorded climatic changes. A number of changes, such as surface subsidence and the degradation of frost mounds due to permafrost thawing have already been observed at many locations.

We surveyed three frost mounds (lithalsas) in the sub-Arctic close to Umiujaq in, northern Quebec, ~~sub-Arctic~~, using ~~a~~ high-precision differential Global Positioning System (d-GPS) technology during field visits in 2009, 2010 and 2011, thus obtaining detailed information on their responses to the freezing and thawing that occurs during the course of the annual temperature cycle. Seasonal pulsations were detected in the frost mounds and these responses were shown to vary with the state of degradation and the land cover. The most degraded lithalsa showed a maximum amplitude of vertical movement (either up or down) between winter (freezing) and summer (thawing) of  $0.19 \pm 0.09$  m over the study period, while for the least degraded lithalsa this figure was far greater ( $1.24 \pm 0.47$  m). Records from patches-areas

1 with little or no vegetation showed far less average vertical movement over the study period  
2 (0.17±0.03 m) than those with prostrate shrubs (0.56±0.02 m), suggesting an influence from  
3 the land-cover.

4 A differential Interferometric Synthetic Aperature Radar (D-InSAR) analysis was also  
5 completed over the lithalsas using selected TerraSAR-X images acquired from April to  
6 October 2009 and from March to October 2010, with a repeat cycle of 11 days.  
7 Interferograms with baselines shorter than 200 m were computed revealing a generally very  
8 low interferometric coherence, restricting the quantification of vertical movements of the  
9 lithalsas. Vertical surface movements of the order of a few centimeters in the centimeter range  
10 were recorded in the ~~near~~-vicinity of Umiujaq.

11

## 12 **1 Introduction**

13 Permafrost underlies 40 - 455% of Canada and is significantly affected by ~~has a significant~~  
14 ~~effect on~~ the global climate. Climate modelling suggests that increasing air temperatures are  
15 to be expected over the next 40 years, with a large increase expected in this area of up to 10°C  
16 during the winter months (Allard et al., 2007). Such elevated air temperatures will affect the  
17 soil temperature, which has been modelled to increase by about 4°C ~~until by~~ 2070 (Sushama  
18 et al., 2006). Such warming would increase thawing during the summer months leading to an  
19 increase in marshlands or wetlands and encouraging the formation of new lakes (Rowland et  
20 al. 2010, Smith et al., 2004).

21 Characteristic landforms of the discontinuous permafrost zone, such as palsas and lithalsas  
22 (Fig. 1 a), are also likely to suffer as a result of increasing soil temperatures, especially as the  
23 ground temperature in these features is usually already >-2°C. Lithalsas are permafrost  
24 mounds; they are typical of northern Quebec and Lapland and are formed by ice segregation  
25 in a similar manner to palsas. In contrast to palsas, however, lithalsas have no insulating cover  
26 of peat (Calmels, 2008; Zoltai and Tarnocai, 1975; Zuidhoff, 2002; Zuidhoff and Kolstrup,  
27 2005), which makes them more sensitive to changes in temperature (Pissart, 2000; Seppälä,  
28 1988). Lithalsas and palsas normally form low circular or oval features that are about 5 m  
29 high, 10-30 m wide, and up to 150 m long. ~~The morphology of lithalsas and palsas are~~  
30 ~~normally low circular or oval features, around 5 m in height, 10-30 m in width and up to 150~~  
31 ~~m in length.~~ The ice lenses of their permafrost cores are usually not thicker than 3 cm, but  
32 lenses up to 40 cm thick have been described (Gurney, 2001; Pissart, 2002). Their anticipated  
33 degradation with continued warming is likely to have severe direct and indirect consequences

1 for the ecosystem, the hydrological regime, and the vegetation, and to ultimately also affect  
2 the human population (Nelson et al., 2003).

3 Changes ~~in the to~~ land surface within the area covered by this study (around Umiujaq in  
4 northern Quebec) over recent years have been attributed to permafrost thawing. A number of  
5 studies (e.g. Laberge and Payette, 1995; Fortier and Aubé-Maurice, 2008) have shown that  
6 longer ~~and~~, warmer summer periods lead to result in degradation of these mounds, ~~(and even~~  
7 ~~their disappearance)~~ accompanied by ~~a~~ subsidence of the surrounding terrain.

8 Increasing temperature and pressure gradients in winter encourage the formation of  
9 segregation ice and cause frost heave. During the thawing period the opposite occurs and  
10 lithalsas subside (Skaven-Haug, 1959). Long-term climatic variations are expected to elicit  
11 responses to changing air temperatures that are comparable to these annual changes. Calmels  
12 et al. (2008), for example, surveyed a lithalsa close to our own study area and recorded thaw  
13 settlement of 1 m over a 5 year period.

14 In this study we have investigated the seasonal dynamics of lithalsas on the eastern shore of  
15 Hudson Bay, in the Nunavik region of northern Quebec, Canada, using a differential system  
16 (d-GPS) and satellite-based differential SAR interferometry (D-InSAR).

17 ~~The d-GPS~~ technology has been successfully used for a wide range of scientific  
18 applications, although ~~its use has only really been used~~ for geocryological purposes ~~only really~~  
19 ~~started in since~~ the mid-~~1990~~'s. For example, Theakstone et al. (1999) ~~generated used d-GPS~~  
20 technology to generate maps and a DEM for a glacier in central Norway, ~~stating claiming~~ a  
21 vertical accuracy of 0.1 m, Kaufmann (1998) ~~evaluated used d-GPS technology to evaluate~~  
22 the stability of reference points on a rock glacier in the Austrian Alps, Tait and Moormann  
23 (2003) found ~~a d-GPS~~ technology to be the best approach for monitoring topographic  
24 movements in continuous permafrost regions, and ~~Sheng-Tait~~ et al. (2004) and Tait et al.  
25 (2005) used ~~a d-GPS~~ technology to survey frost mounds within the continuous permafrost  
26 zone. A number of research teams have also successfully used ~~a d-GPS~~ technology to monitor  
27 frost heave and thaw subsidence. For example, Little (2006), Little et al. (2003) and Nelson et  
28 al. (2001) collected d-GPS measurements in flat areas of northern Alaska, where they  
29 recorded heave and subsidence movements of up to 0.06 m. Shiklomanov et al. (2013) used a  
30 d-GPS to quantify isotropic thaw subsidence in permafrost areas of northern Alaska, and Wirz  
31 et al. (2015) derived the temporal variability of mountain permafrost slopes using d-GPS  
32 measurements.

1 In addition to field measurements, remotely-sensed radar data has also been used to detect  
2 vertical movements in permafrost regions from space, by means of differential interferometry.  
3 Differential Interferometry Synthetic Aperture Radar (D-InSAR) uses the phase content of a  
4 complex radar signal to detect land surface deformations by transforming the phase difference  
5 between two acquisitions into a displacement figure (e.g. Bamler and Hartl, 1998). Changes  
6 of the order of centimetres, or even millimetres, can be observed depending on the sensor's  
7 wavelength. Such an analysis requires at least two scenes of the area of interest, recorded by  
8 the same sensor but at different times, and an appropriate digital elevation model (DEM). D-  
9 InSAR has mainly been used to detect large-scale deformations caused by earthquakes (e.g.  
10 Yen et al., 2008) or by seismic and volcanic activities (e.g. Ge et al., 2008; Amelung et al.,  
11 2000), but it has also been used to monitor glacier velocity (e.g. Goldstein et al., 1993). The  
12 first extensive studies of permafrost thawing and freezing in the Arctic (North Slope of  
13 Alaska) using D-InSAR were based on data from the ERS SAR sensor (C-band, 5.7 cm  
14 wavelength) (Liu et al., 2010; Liu et al., 2011). Data has also been available at a higher spatial  
15 resolution since 2006 from COSMO-SkyMed (ASI, 2007), based on shorter wavelengths (X-  
16 band 3.6 cm), and since 2007 from the TerraSAR-X satellite (DLR, 2010). A number of  
17 studies have since been initiated using TerraSAR-X data to investigate vertical movements  
18 caused by permafrost thawing within the Arctic region (Larsen et al., 2009; Larsen et al.,  
19 2011; Lauknes et al., 2010a; Lauknes et al., 2010b; Short et al., 2011; Short et al., 2014;  
20 Strozzi et al., 2012).

21 Little is known about the surface movements of frost mounds (lithalsas), in particular about  
22 their responses to the freezing and thawing that occurs during the course of an annual  
23 temperature cycle, or the relationship between these movements and the state of degradation  
24 of the frost mounds or their vegetation cover. We therefore surveyed three lithalsas in the  
25 Canadian sub-Arctic using d-GPS technology to obtain more detailed information. In order to  
26 investigate the use and effectiveness of new and innovative technologies we also used D-  
27 InSAR data which, to the author's best knowledge, has not previously been used to investigate  
28 this type of permafrost landform. We analyzed TerraSAR-X images acquired between April  
29 2009 and October 2009 and between March and October 2010, with a repeat cycle of 11 days,  
30 from which we obtained valuable information concerning the possibility of using D-InSAR in  
31 this kind of environment.

32

## 33 **2 Study area description**

1 The study area covers about 60 km<sup>2</sup> and is located near the Inuit village of Umiujaq (56°33'  
2 N, 76°33' W), close to the eastern shoreline of Hudson Bay in Nunavik, northern Quebec,  
3 Canada (Fig. 2).

4 The study area is located in the transition zone between the sub-Arctic and the Arctic, where a  
5 high sensitivity to climatic changes is expected making it an ideal region in which to conduct  
6 a climate change impact study. The permafrost is ~~mainly scattered~~sporadic (Fig. 2) and the  
7 study area covers the northern timber line; the mean annual ground temperature (MAGT) at a  
8 depth of 10 m is about -2.5°C (Smith et al., 2010).

9 There are currently only 60 to 80 frost-free days per year in the study area (Environment  
10 Canada, 2004) and the annual average air temperature is about -5.5°C but, due to the  
11 proximity of Hudson Bay, the region is characterized by high temperature variability  
12 throughout the year. From June until mid-December the climate has a maritime character with  
13 little diurnal variation in temperature and moderate temperatures of about 8°C. In contrast,  
14 when Hudson Bay freezes over during the winter temperatures can reach to below -30°C due  
15 to continentality. In addition, the annual average wind speeds in this area are between 20 and  
16 24 km/h (Gagnon and Ferland, 1967), resulting in wind-chill temperatures down to -60°C  
17 (Environment Canada, 2004). The average annual precipitation is approximately 500 mm  
18 (Phillips, 1984), of which 37% falls as snow (Environment Canada, 2004).

19 The study area can be divided into a coastal region with gently sloping topography and the  
20 Lac-Guillaume-Delisle graben (Fig. 2). The two landscape units are separated by ridges of  
21 outcropping bedrock (consisting of volcanic sediments) known as 'Cuestas' (Kranck, 1951).  
22 The entire study area is experiencing a heterogeneous post-glacial rebound that averages  
23 about 1.0 cm/year (Lajeunesse and Allard, 2003; Tait and Moorman 2003).

24 Temperatures in the region around Umiujaq are expected to increase by up to 10°C over the  
25 next 40 years, with the rate of increase expected to be highest during the winter months  
26 (Allard et al., 2007). Such an increase in air temperature would have an impact on the soil  
27 temperature, which would in turn be expected to increase by approximately 4°C by 2070).  
28 These modelling results obtained by Sushama et al. (2006) suggest a significant future  
29 deepening of the active layer, which would be likely to result in thaw-related settlement  
30 (Calmels, 2008).

31

### 32 **3 Data and methods**

1 The data used for this study consisted of information collected during field visits in 2009,  
2 2010 and 2011, together with remotely sensed data acquired by the German TerraSAR-X  
3 satellite. The *in-situ* measurements provided detailed information on the seasonal variations in  
4 lithalsas at specific locations and were also used to validate the results obtained from analysis  
5 of the remote sensing data. Table 1 shows the acquisition dates for the d-GPS and TerraSAR-  
6 X data, as well as details ~~the dates~~ of the useable differential interferograms. Thaw depths  
7 were also measured at the same time as the other field measurements were obtained, using a  
8 frost probe.

### 9 **3.1 Field data**

10 The three lithalsas investigated (identified as I, R, and M) are located to the south-east of the  
11 community of Umiujaq (Fig. 3)

12 They are each about 40 m in diameter and between 5 and 10 m high. They comprise a mixture  
13 of patches of bare ground and areas covered by lichens or prostrate shrubs, with their slopes  
14 being covered in small shrubs. A detailed soil map (1:10,000 scale) by Doyon et al. (2010)  
15 identifies the three features as ice-rich frost mounds ('Buttes cryogènes riche en glace').  
16 Lithalsas I and R lie within a zone of aeolian sediments dominated by sand, sandy silt, sandy  
17 gravel and gravel ('Sable, silt sableux, sable graveleux et gravier'). Lithalsa M is further to  
18 the south-east in an area of marine and littoral sediments consisting mainly of sand but  
19 including beds of heavy minerals and shell fragments ('Sable moyen à grossier avec présence  
20 de lits de minéraux lourds et de fragments de coquillages'). Adjacent to the southern slope of  
21 this lithalsa lies a poorly drained wetland area (Doyon et al., 2010).

22 The three lithalsas all exhibit clearly different states of degradation. A 220 m<sup>2</sup> pond on the  
23 eastern side of Lithalsa R provides evidence that this lithalsa is in the process of breaking up,  
24 with additional evidence coming from the presence of numerous cracks and small-scale  
25 solifluction features (Fig. 1b). A pond has also formed on the north-east-facing slope of  
26 Lithalsa M, but its dimensions are smaller (Fig. 3) and there are far fewer cracks than at  
27 Lithalsa R. Degradation at Lithalsa M is therefore interpreted to be less advanced than at  
28 Lithalsa R. There is, in contrast, no evidence of degradation at Lithalsa I, which has no pond  
29 and no visible cracks. Table 2 summarizes the characteristics of the three lithalsas.

30 Seven field visits were made between August 2009 and April 2011, covering the full range of  
31 seasons. The three lithalsas were surveyed using a ProMark 3 GPS from Magellan with a  
32 NAP100-L1 antenna. The d-GPS technology allows accurate measurement of vertical  
33 movements (at centimeter or even sub-centimeter scales) within a worldwide geodetic

1 coordinate system. This is achieved using normal code-based GPS technology, which acquires  
2 coordinate positions through triangulation by defining the interspace between at least four  
3 satellites and a receiver (UNVACO, 2006). This kind of GPS only has an accuracy of a few  
4 meters, but this is improved by using a differential system (d-GPS) equipped with at least two  
5 receivers. One of the two receivers serves as the base station: it has a known (fixed) position  
6 from which it tracks the satellites. The other receiver (the rover receiver) is placed at a  
7 particular point for only a limited period of time (usually between 15 and 60 seconds;  
8 [http://www.trimble.com/gps\\_tutorial/](http://www.trimble.com/gps_tutorial/)). By comparing the signals from the two receivers at the  
9 same point in time, systematic errors, such as those due to atmospheric signal delays or ~~the~~  
10 variations in the precision of the orbits, can be substantially reduced (Trimble, 2010). For this  
11 the "kinematic stop-and-go d-GPS method" (Berber et al., 2002) was used. Hofmann-  
12 Wellenhof et al. suggested that the best accuracy was achieved with this method if the phase  
13 ambiguities were resolved before starting the survey. This we achieved through the use of a  
14 static initialization process provided by Magellan in their initialization equipment. The  
15 numbers recorded by the d-GPS were stored in RINEX (Receiver Independent Exchange)  
16 format. The data were analysed using the GNSS Solution v3.10.07 post-processing software  
17 (Magellan), with the data being imported into the software and then processed by adjusting  
18 vectors in relation to a fixed control point received from the base station.

19

20 ~~The records were analysed using GNSS Solution v3.10.07 post-processing software, also~~  
21 ~~from Magellan.~~ Coordinates and elevations for the 39 measurement points (R1 – R12, M1 –  
22 M14, and I1 – I13) over the three lithalsas were determined in August 2009, March 2010,  
23 May 2010, August 2010, and April 2011. The base station was mounted, always mounded at  
24 the same location, about 500 m from the lithalsas, ~~close to at a marked~~ trigonometric point on  
25 stable bedrock where changes in elevation caused by frost heave or thawing subsidence could  
26 be excluded. Unfortunately ~~however, the original details of this trigonometric point could not~~  
27 ~~be obtained. the trigonometric point could not be identified~~ and, due to the remoteness of the  
28 study area no permanent reference station was available. Since this introduced the possibility  
29 of errors in the recorded position of the base station, the measured coordinates needed to be  
30 manually corrected for each record date before running the post-processing software. This  
31 correction was undertaken using the online service provided by the NRCan's Geodetic Survey  
32 Division ([www.geod.nrcan.gc.ca/index\\_e.php](http://www.geod.nrcan.gc.ca/index_e.php)) in which the recorded coordinates are  
33 submitted to the system, together with information concerning the processing mode and the  
34 reference system. The Precise Point Position (PPP) is then calculated based on the Canadian  
35 Spatial Reference System (CSRS) (Bisnath and Gao, 2009). The coordinates finally defined  
36 by the CSRS for the base station were 56.55° N and 76.54° E. These coordinates then served  
37 as a control point for the processing described above. Both horizontal and vertical  
38 uncertainties were calculated during post-processing. The horizontal error was found to be

1 between 0.001 cm (Lithalsa M) and 0.098 cm (Lithalsa R), and the vertical error between  
2 0.001 cm (Lithalsa M) and 0.123 cm (Lithalsa I).

3 The points on the three lithalsas at which measurements were to be recorded by the mobile  
4 receiver were first selected in August 2009. It was important to ensure that they were located  
5 within snow-free areas and in either non-vegetated patches or sparsely vegetated patches  
6 (with lichens and/or prostrate shrubs). The selected points were marked with a metal-pin  
7 about 20 cm long, hammered into the ground and wrapped with pink tape.

8 The Magellan user's guide states that a vertical accuracy of "up to" 1.5 cm is attainable when  
9 using a recording time of at least 15 seconds, and that this may be improved by using longer  
10 recording times. For this study a recording time of 60 seconds at each point was chosen and  
11 since there were no obstacles interrupting the signal this should ideally have resulted in an  
12 accuracy of several millimetres. However, because of the need to compute a correction for the  
13 coordinates of the base station (~~see details below~~), the vertical accuracy was reduced to within  
14 a few centimetres (~ 5 cm).

### 15 **3.2 Remote sensing data**

16 In addition to the ground measurements, contemporaneous records from the TerraSAR-X  
17 satellite were also examined. Launched in June 2007, this satellite acquires high-quality X-  
18 band radar images with a spatial resolution of down to 1 m whilst circling the earth in a polar  
19 orbit at an altitude of 514 km. The frequency that the X-band sensor operates at is 9.65 GHz,  
20 which corresponds to a wavelength of about 3 cm (DLR, 2010). Its repetition time is 11 days.  
21 There are several acquisition modes available and we based our choice of the most suitable  
22 mode on coherence images computed from more than 30 images acquired in 2009 on different  
23 passes, at different polarizations, and with different angles of incidence. We considered only  
24 images acquired in the StripMap mode, scanning the surface with a footprint of 30 x 50 km  
25 and a spatial resolution of about 3 m (Table 32), in order to obtain the best possible  
26 compromise between maximum spatial resolution and maximum coverage~~in order to~~  
27 ~~compromise the best spatial resolution and the best coverage~~. Our investigations indicated that  
28 data from an ascending pass, in VV polarization and with an incidence angle of 40° was the  
29 most suitable for the study (Spannraft, 2010; May, 2011). Interferograms computed from  
30 winter acquisitions could not be considered, because snow influenced the radar signal  
31 resulting in too few coherences to process.

32 TerraSAR-X interferograms were computed using a 1-look in "range" and 1-look in  
33 "azimuth", in order to achieve the best possible resolution over the lithalsas. A very high

1 resolution DEM was used for the differential interferometry, in a two-pass approach (Bamler  
2 and Hartl, 1998). The DEM was produced by the Direction de la cartographie topographique  
3 du ministère des ressources et de la faune à Québec (MRNF) from stereoscopic analysis of  
4 aerial photographs, and has a spatial resolution of 1 m. GAMMA Software (GAMMA Remote  
5 Sensing AG, 2008) was used for the processing and an area of 62000 x 25000 pixels defined  
6 for the calculation of the differential interferograms. In order to support phase unwrapping  
7 and as a measure of the quality of the interferograms, coherence was estimated using an  
8 adaptable window from the 1-look differential SAR interferograms (Wegmüller and Werner,  
9 1996). The coherence was first estimated using a fixed, relatively small window size of 15  
10 pixels. The window size was then determined from the first estimate, applying successively  
11 larger windows up to 45 pixels in order to estimate lower coherence. This procedure enabled  
12 us to obtain reliable coherence values without compromising too much on the spatial  
13 resolution.

14 The differential interferograms, which in their initial stage only contained information on the  
15 phase difference, were then unwrapped using the minimum cost flow algorithm in order to  
16 retrieve vertical displacement (Constantini and Rosen, 1999). The high resolution DEM was  
17 also used for georeferencing.

18

## 19 **4 Results and discussion**

### 20 **4.1 Field measurements – differential GPS (d-GPS)**

#### 21 Results

22 The field measurements showed a similar pattern at most of the measurement points, with  
23 88.9% of these points recording uplift during freezing periods (after August 2009 – March  
24 2010: average uplift 0.44 m; August 2010 – April 2011: average uplift 0.11m) and subsidence  
25 during thawing (March 2010 – August 2010: average subsidence 0.46 m). The vertical  
26 movements at those measurement points that did not conform to this pattern were small  
27 (average: 0.1 m) compared to the average vertical movement of all points of 0.4 m between  
28 August 2009 and April 2011.

29 Figure- 4 shows the heights of the lithalsa surfaces (both an average height for all three  
30 lithalsas and separate heights for each lithalsa, averaged from all the relevant measurement  
31 points) over the 20 month period relative to the height of the base station, measured on 6  
32 different dates (14.08.2009, 25.03.2010, 08.05.2010, 12.08.2010, 27.10.10, and 09.04.2011)  
33 and interpolated over the entire 20 month period. It should be pointed out that for October

1 2010 observations were only available from Lithalsa I due to the weather conditions that did  
2 not allow further measurements.

3 The average heights (black bars) increase by 0.44 m between August 2009 and March 2010,  
4 followed by a rapid decrease between March 2010 and May 2010 of 0.32 m, with a further  
5 decrease of 0.14 m to August 2010, followed in turn by a slight increase of 0.10 m to April  
6 2011. The difference between the highest average elevation (March 2010) and the lowest  
7 average elevation (August 2010) was 0.47 m. Between March 2010 and May 2010 an average  
8 subsidence across all lithalsas of 0.35 m was recorded, which represents 70.6 % of the total  
9 subsidence over the entire year 2010. The subsequent average subsidence across all lithalsas  
10 between May 2010 and August 2010 was far less (0.12 m) even though the period was nearly  
11 2 months longer.

12 ~~These records clearly confirm the expected seasonal frost heave and thaw subsidence, and~~  
13 ~~also indicate that that these processes are not linear over the whole year: the frost heaving~~  
14 ~~during the freezing period (after August 2009 – April 2010) was rather slow compared to the~~  
15 ~~rapid subsidence following the initial thaw in late April or May. The freezing process~~  
16 ~~therefore seems to operate much more slowly than the thawing process. The very minor frost~~  
17 ~~heave observed during the 2010-2011 freezing period (average across all lithalsas: 0.04 m)~~  
18 ~~was not as pronounced as in the previous (2009-2010) freezing period. Possible reasons for~~  
19 ~~this difference are discussed later in this section.~~

20 The relative heights of the individual lithalsas (grey bars) all show similar trends but the  
21 amplitudes of their vertical movements vary considerably: Lithalsa R shows the least  
22 variation in height over time (August 2009 – April 2011), with the maximum recorded  
23 vertical movement being the subsidence of 0.19 m between March 2010 and August 2010. All  
24 recorded vertical movements totaled over the entire period and averaged over all  
25 measurement points on Lithalsa R amount to 0.48 m. The net movement of lithalsa R amount  
26 to 0.06 m.

27 The maximum recorded vertical movement averaged across all measurement points on  
28 Lithalsa M was 0.20 m (between May 2010 and August 2010), and the total vertical  
29 movement (as for Lithalsa R) was 0.57 m. Lithalsa M reached its maximum uplift two months  
30 later than the other lithalsas.

31 Lithalsa I showed much greater vertical movement over the year than the other lithalsas, with  
32 a dramatic peak in its relative height in March 2010 followed by a very rapid decrease to May  
33 2010. The greatest vertical movement (1.24 m) occurred between August 2009 and March

1 2010, and the sum of all vertical movement (as above) over the entire period was 3.2 m.  
2 Lithalsa I is the only lithalsa for which records are available from October 2010. The net  
3 movement at ~~Lithalsa I is with~~(-0.01m) ~~was~~ again less than the net movement at the other two  
4 lithalsas.

5 Analyzing the measurements from individual measurement points (Fig. 3) reveals that the  
6 smallest vertical movement occurred at a point on Lithalsa R (R3), which had less than 0.2 m  
7 total movement over the 20 months period. The largest vertical movements (i.e. the  
8 summations of all movements at each location~~of over~~ the 20 month period) occurred ~~on~~  
9 ~~at~~Lithalsa I, at I4 (5.7 m) and I5 (6.0 m). ~~on-~~ Lithalsa I. These high numbers on Lithalsa I are  
10 largely due the rapid subsidence that occurred between March and May 2010. Observations  
11 from the R12 point indicate continuous subsidence during this period. This behavior is  
12 probably due to the location of R12 on at the outer slope of the lithalsa (Fig. 3), where  
13 advanced degradation is evident in the form of cracks and solifluction~~occurs~~.

14 Taking into account the different trends over the 20 month period as well as the behavior at  
15 the individual measurement points, it is clear that Lithalsa I was the most dynamic lithalsa  
16 over the observation period, while Lithalsa R was the least dynamic. Lithalsa I was not only  
17 the most dynamic at all of the measurement points but also showed the greatest amount of  
18 variation between the measurement points. Hence, as far as the seasonal behavior of the frost  
19 mounds is concerned, the lithalsa with the least evidence of degradation (Lithalsa I) is the  
20 most active of the three lithalsas while Lithalsa R, which shows the most advanced signs of  
21 degradation, is the least active.

22

## 23 Discussion

24 The records clearly confirm the expected seasonal frost heave and thaw subsidence and reveal  
25 a correlation between a lithalsa's degradation and its seasonal variations. They also indicate  
26 that that these processes do not operate in a linear manner over the whole year: the frost  
27 heaving during the freezing period (starting after August 2009) was rather slow compared to  
28 the rapid subsidence that followed the initial thaw in late April or May. The freezing process  
29 therefore seems to operate much more slowly than the thawing process. The very minor frost  
30 heave observed during the 2010-2011 freezing period (average across all lithalsas: 0.04 m)  
31 was not as pronounced as that observed during the previous (2009-2010) freezing period.

32 ~~Our results all conform to the expected seasonal variations in the elevation of lithalsas over~~  
33 ~~the course of a year; they also reveal the correlation between a lithalsa's degradation and its~~  
34 ~~seasonal variations. However, the relatively small amount of uplift in all three lithalsas~~

1 | ~~between the fall of 2010 and April 2011 requires some explanation.~~ The possibility of early  
2 | thawing in 2011 having already resulted in any subsidence by April can be discounted as air  
3 | temperatures were still well below 0°C (the average air temperature for January to April, 2011  
4 | was -16°C; CEN, 2013). There are, however, two other possible explanations: (i) maximum  
5 | thawing had probably not yet been reached in August 2010, which would mean that the  
6 | lithalsas were still in the process of subsiding (as suggested by the observations from Lithalsa  
7 | I in October 2010, which show further subsidence of 0.03 m since August 2010), and (ii) the  
8 | late initiation of freezing in 2010, when air temperatures did not drop permanently below 0°C  
9 | until the 17<sup>th</sup> of November which is almost one month later than in 2009 (20<sup>th</sup> October: CEN,  
10 | 2013), is likely to have delayed the uplift process, which was therefore possibly not yet  
11 | completed in April 2011.

12 | A detailed analysis of each individual measurement point yielded additional information: the  
13 | low average increase in elevation recorded between August 2010 and April 2011 is due to  
14 | 35% of the measurement points actually experiencing subsidence rather than elevation. Five  
15 | of these points in particular (R6, R9, R11, M4, and M13) showed a great deal of subsidence  
16 | (averaging -0.19 m) and were therefore largely responsible for the low average uplift. The  
17 | seasonal uplift (frost heave) trend is thus dampened by just 13% of the measurements that  
18 | exhibit high counter-trends (i.e. subsidence). If these 5 points are ignored the average uplift  
19 | amounts to almost 0.1 m.

20 | In order to better understand the behavior at individual measurement points we also took into  
21 | account the vegetation and noted that 93% of the subsiding points were either vegetation-free  
22 | or covered only with ~~a small few patches of amount of~~ lichen. Thirteen of the fourteen  
23 | measurement points that recorded subsidence between August 2010 and April 2011 also  
24 | experienced below-average frost heave in the preceding winter of 2009-2010. ~~Overall,~~ 85% of  
25 | the points with below average least uplift were either mostly covered with lichen or non-  
26 | vegetated. Those measurement points with above average uplift (>61% of all measurement  
27 | points in the winter of 2009/2010 and >83% of all measurement points in the winter of  
28 | 2010/2011) were covered with prostrate shrubs. A similar observation can be made for the  
29 | summer thawing process (May 2010 – August 2010): 78% of the points with below average  
30 | subsidence (14 out of 39) were either covered with lichen or non-vegetated, while (88%) of  
31 | the points experiencing with above average subsidence (25 out of 39) were covered with  
32 | prostrate shrubs. Between March 2010 and May 2010 none of the non-vegetated or lichen-  
33 | covered measurement points showed above-average subsidence, but most (80%) of these  
34 | points showed either continuing uplift or minor subsidence. ~~Patches Areas~~ with prostrate

1 shrubs therefore clearly start to subside earlier than those with little or no vegetation. In view  
2 of the weather in the spring of 2010, temporary early thawing is a real possibility as there had  
3 already been 17 days, with temperatures of up to 6°C (reached on 31<sup>st</sup> March 2010; CEN,  
4 2013); before the survey was conducted (8<sup>th</sup> of May, 2010).

5 The lower overall dynamics at non-vegetated measurement points is not surprising since the  
6 records of the active-layerthaw depths in-during the same year (2010) indicate that non-  
7 vegetated areas had very thin-shallow (<5-60 cm) thaw depths in the summer (August)  
8 compared to patches areas covered with shrubs or trees, where the thaw depth was -up to 200  
9 m (Beck et al., 2015). This is due to the absence of any insulation during the winter (i.e. no  
10 insulating cover of either vegetation or snow), resulting in lower ground temperatures (e.g.  
11 Beck et al. 2015; Clebsch and Shanks, 1968; Mackay, 1974; Romanovsky and Osterkamp,  
12 1995; Nelson et al., 1997). It can therefore be assumed that subsidence at these points starts  
13 much later than elsewhere. The relationships between the different vegetation types and the  
14 changes in elevations changes is-are shown in Figure- 5.

15 Both the vegetation and the snow cover influence the thermal regime of the ground. However,  
16 since frost mounds are exposed features in the landscape any snow cover is usually quickly  
17 removed by the wind and they are commonly almost frost free (Fig. 6). The influence of snow  
18 cover on the mounds has therefore not been included in this study.

## 19 **4.2 Remote sensing - Differential Interferometry Synthetic Aperture Radar (D- 20 InSAR)**

### 21 Results

22 Out of the 11 TerraSAR-X acquisitions in 2009 and 2010, only six interferograms showed a  
23 reasonable coherence with coherence values greater than about 0.25 computed over the whole  
24 area of interest (i.e. 0.23 for the 7 May/14 August 2009 image pair, 0.40 for the 14 August/30  
25 August 2009 pair, 0.29 for the 14 August/30 October 2009 pair, 0.27 for the 5 May/12 August  
26 2010 air, 0.53 for the 12 August/28 August 2010 pair, and 0.28 for the 12 August/28 October  
27 2010 pair). All other interferograms were much less correlated. Areas covered by water  
28 bodies, vegetated areas, and pixels located within shadows are particularly affected by  
29 decorrelation with coherence values below 0.3, while built-up areas are by far the most  
30 coherent class, with coherence values greater than 0.9. However, although the average  
31 coherence value from the six interferograms is high enough for generalised further analysis  
32 (Carballo and Fieguth, 2002; Hanssen, 2001), the coherence values over the three lithalsas

1 (Table 4) is too low to be considered adequate for further analysis. In this case, if phase  
2 unwrapping is performed without using a coherence threshold it will yield phase values  
3 approaching zero, which would be typical of noisy regions. However, these values show no  
4 correlation with the large displacements measured using d-GPS technology and have therefore  
5 not been subjected to any further analysis.

## 6 7 Discussion

8 Decorrelation in the TerraSAR-X differential interferograms over the lithalsas (Fig. 7a) is not  
9 surprising considering the large, rapid, vertical movements (several decimeters in less than  
10 half a year) measured using d-GPS technology (Zebker & Villasenor). There are also large  
11 variations in movement within each of the lithalsas. Amplitudes of several decimeters in  
12 lithalsa movements were recorded over less than half a year, with variations of several  
13 centimeters between individual measurement points within each of the lithalsas (which are  
14 only about 40 m in diameter); these amplitudes far exceed the the range that can be quantified  
15 with TerraSAR-X data, where a phase cycle corresponds to 1.6 cm and the time interval  
16 between acquisitions is, at best, 11 days. Decorrelation due to large displacements resulting  
17 from freeze-up processes has also been identified by Short et al. (2011), when they tried to co-  
18 register TerraSAR-X and RADARSAT-2 data from Herschel Island, acquire in May, October  
19 and November. The possibility of temporal decorrelation associated with the land cover type  
20 can be discounted because the lithalsas have only very sparse vegetation cover, or none at all,  
21 as is also the case in surrounding areas that are characterized by much higher coherence  
22 values (Fig. 7b). Changes in the dielectric properties (soil and vegetation moisture) can also  
23 influence both the coherence and the phase (Barrett et al., 2012). However, investigations in  
24 Canadian permafrost regions (Pangnirtung and Iqaluit) by Short et al. (2014) examined the  
25 influence of soil moisture and found that it was unlikely to be a significant source of error  
26 Nevertheless the six differential interferograms reveal two interesting large scale signals.  
27 Firstly, to the north of Umiujaq (56°33.6' N, -76°32.94'E) fringes increase with time and may  
28 be an indication of localized slow movements in a rocky area with only sparse vegetation  
29 (such as lichens and mosses). A corner reflector was fixed on solid rock in this area by INRS  
30 for a RADARSAT-2 study, oriented for a descending orbit. The signal in the TerraSAR-X  
31 interferograms could be related to localized movement of the corner reflector, to the  
32 displacement of terrain relative to the corner reflector, or to thermal dilation associated with  
33 the structure on which the corner reflector is located. It is not possible to make any further  
34 interpretations concerning the cause of the detected movement without additional local

1 information. Secondly, to the west of the lithalsas (around 56°33.18'N, -76.30.96'E),  
2 widespread slow movements can be identified over the 11 day period from 14 to 23 August  
3 2009. This area is part of the Cuestas (solid rock) but land cover classifications based on an  
4 IKONOS image (2005) and a GeoEye image (2009) show vegetated patches with prostrate  
5 shrubs (May, 2011), interspersed with temporary pools of water. Following the signals from  
6 the differential interferogram are therefore very likely to be associated with temporary  
7 ponding. This interpretation is supported by the precipitation records: 63% of the total  
8 precipitation for August (total: 64.4 mm) fell between the two acquisition dates (i.e. between  
9 14.08.2009 and 30.08.2009), whereas it was very dry (only 5.8 mm precipitation) over the  
10 seven days prior to the first acquisition.

11

## 12 **5 Conclusion**

13 ~~The dD-GPS records-measurements have~~ confirmed the expected vertical movements of  
14 lithalsas relatively to the surrounding unfrozen ~~environment-ground-around-them.~~ The average  
15 uplifts during the two freezing periods (winter 2010 and winter 2011) measured ~~with-using~~ d-  
16 GPS technology are-were 0.4 m and 0.1 m. The average measured subsidence during the  
17 thawing period (summer 2010) ~~is-was~~ 0.5 m. The results ~~also~~ indicate different patterns of  
18 behavior for each of the three lithalsas, reflecting their degradation status: maximal  
19 movements were recorded for the ~~less-least~~ degraded lithalsa (21% above the average) and  
20 minimal movements were recorded for the most degraded lithalsa (40% below the average).  
21 With regard to the vegetation cover, patches with prostrate shrubs cover experienced greater  
22 uplift and subsidence than those with little or no vegetation. The amount of movements ~~also~~  
23 ~~shows~~indicates that permafrost features in this region are currently undergoing active  
24 degradation. Furthermore, the results and interpretations from our research using d-GPS  
25 technology in sub-Arctic permafrost regions will have important implications for planning the  
26 use of D-InSAR in such regions, and for interpreting the results obtained.~~Furthermore the d-~~  
27 ~~GPS implications and experiments in sub-Arctic permafrost regions and the achieved results~~  
28 ~~are very important for the planning of D-InSAR experiments and the understanding of D-~~  
29 ~~InSAR in sub-Arctic regions. As~~ Since in-situ subsidence data ~~in-from this-such~~ environments  
30 is very rare, D-InSAR analysis is often performed without a-priori knowledge. However  
31 ~~Though, t~~hese movements could not be detected with D-InSAR due to decorrelation. ~~It-could~~  
32 ~~be-shown-that~~ large displacements ~~can-occur~~have been shown to be possible, which makes  
33 the application of D-InSAR in ~~this-such~~ regions very challenging. This became evident ~~by-as~~

1 | ~~a result of~~ capturing the ~~lithalsas'~~ dynamics ~~of lithalsas~~ in the differential interferograms  
2 | based on the X-band data ~~of from~~ TerraSAR-X. This investigation therefore revealed the  
3 | limitations of ~~D-InSAR this method, as since~~ the range of movements (several cm) could not  
4 | be represented in the D-InSAR products. However, slow movements could be identified in the  
5 | general vicinity, ~~to the~~ north of Umiujaq and east of the lithalsas. These findings are of ~~high~~  
6 | ~~considerable~~ importance as they confirm the usability of D-InSAR based on X-band to detect  
7 | vertical dynamics in sub-Arctic regions.

## 8 | **Author contributions**

9 | I. Beck was responsible for the design of the experiments, the field work, ~~and~~ the generation  
10 | of the D-InSAR products, as well as ~~for~~ the analysis and interpretation of the results. R.  
11 | Ludwig and M. Bernier ~~were supervising supervised~~ her work and ~~assisted provided assistance~~  
12 | her during the study. S. Tazio supported the preparation of the D-InSAR products and the  
13 | analysis. J. Boike was responsible for the interpretation of the permafrost processes. All co-  
14 | ~~authors authors have~~ supported I. Beck ~~with in~~ the preparation of the manuscript.

## 15 | **Acknowledgments**

16 | The authors gratefully acknowledge the financial support received from ArcticNET, the DFG  
17 | (Deutsche Forschungsgemeinschaft), the CEN (Centre d'études nordiques), and the European  
18 | Union FP7-ENV project PAGE21 under contract number GA282700. We are also grateful to  
19 | the DLR-HR for providing the remote sensing data, to GAMMA Remote Sensing AG for  
20 | their technical support, and to Yannick Duguay (Ph.D. at CEN) for assistance with ~~the~~ d-GPS  
21 | data acquisition.  
22 |  
23 |

## 1 **References**

- 2 Allard, M., and Séguin, M.K.: Le pergélisol au Québec nordique: bilan et perspectives. *Géogr*  
3 *Phys Quatern*, 41, 141–152, 1987.
- 4 Allard, M., Fortier, R., Sarrazin, D., Calmels, F., Fortier, D., Chaumont, D., Savard, J.P., and  
5 Tarussov, A. : L’impact du réchauffement climatique sur les aéroports du Nunavik :  
6 caractéristiques du pergélisol et caractérisation des processus de dégradation des pistes.  
7 Sommaire Project A803. University Laval, Ouranos, Canada, 2007.
- 8 Amelung, F., Jónsson, S., Zebker, N. and Segall, P. : Widespread uplift and ‘trapdoor’  
9 faulting on Galápagos volcanoes observed with radar interferometry. *Nature*, 407, 993-  
10 996, 2000.
- 11 ASI (Italian Space Agency) : COSMO-SkyMed Mission, COSMO-SkyMed System  
12 Description & User Guide, Rome, Italy, 2007.
- 13 Bamler, R., and Hartl, P. : Synthetic aperture radar interferometry. *Inverse Problems*, 14, R1 –  
14 R54, 1998.
- 15 [Barrett, B., Whelan, P., and Dwyer, E.: The use of C- and L-band repeat-pass interferometric](#)  
16 [SAR coherence for soil moisture change detection in vegetated areas. \*The Open Remote\*](#)  
17 [\*Sensing Journal\*, 5 \(1\), 37-53, 2012.](#)
- 18 Beck, I., Ludwig R., Bernier, M., Lévesque, E., and Boike, J.: Assessing permafrost  
19 degradation and land cover changes (1986-2009) using remote sensing data, Umiujaq,  
20 sub-Arctic Quebec. *Permafrost Periglac*, doi:10.1002/ppp.1839, online first, 2015.
- 21 [Berber, M., Ustun, A., and Yetkin, M.: Comparison of accuracy of GPS techniques.](#)  
22 [\*Measurement\* 45, 1742-1746, 2012.](#)
- 23 [Bisnath, S., and Gao, Y.: Current State of Precise Point Positioning and Future Prospects and](#)  
24 [Limitations, in: \*International Association of Geodesy Symposia Volume 133\*, 615-623,](#)  
25 [2009.](#)
- 26 Calmels, F.: Genèse et structure du Pergélisol. Etude de forms périglaciaires de soulèvement  
27 au gel au Nunavik (Québec nordique), Ph.D. thesis, Department. of Geography,  
28 Université Laval, Quebec, Canada, 169 pp., 2008.
- 29 Calmels, F., Allard, M., and Delisle G. : Development and decay of a lithalsa in Northern  
30 Québec: A geomorphological history. *Geomorphology*, 97, 287-299, 2008.

1 CAF – Cluster Applied Remote Sensing-: TerraSAR-X. Ground Segment. Basic Product  
2 Specification Document. Oberpfaffenhofen, Germany, 2009.

3 Carballo, G.F., and Fieguth. P.W.-: Member hierarchical network flow phase unwrapping.  
4 IEEE Geosci Remote S, 40, 1695-1708, 2002.

5 CEN: Environmental data from the Umiujaq region in Nunavik, Quebec, Canada, v. 1.1  
6 (1997-2013). Nordicana D9, doi: 10.5885/45120SL-067305A53E914AF0, 2013.

7 Clebsch, E.E.C., and Shanks, R.E.: Summer climatic gradients and vegetation near Barrow,  
8 Alaska. Arctic, 21, 161-171, 1968.

9 Constantini, M., and Rosen P.A. : A generalized phase unwrapping approach for sparse data,  
10 in-: Proceedings IGARSS, Hamburg, Germany, 28. June – 02. July 1999, 267-269, 1999.

11 Doyon, J. R., Allard, M., and L’Hérault E. : Umiujaq, Dépôts de surface, aéroport ‘Umiujaq,  
12 Nunavik. Centre d’études nordiques, Université Laval, Québec, Canada 2010.

13 DLR : [http://www.dlr.de/eo/desktopdefault.aspx/tabid-5725/9296\\_read-15979/](http://www.dlr.de/eo/desktopdefault.aspx/tabid-5725/9296_read-15979/), last access-:  
14 20.January 2010.

15 Environment Canada : Canadian Climate Normals, 1971-2000. Environment Canada,  
16 Atmospheric Environment Service, Ottawa, Ontario, Canada, 2004.

17 Fortier R., -and Aubé-Maurice B.-: Fast Permafrost Degradation near Umiujaq in Nunavik  
18 (Canada) Since 1957 assessed from Time-Lapse Aerial and Satellite Photographs, in:  
19 Proceedings of the Ninth International Conference on Permafrost, 29 June – 3 July 2008,  
20 University of Fairbanks-: Fairbanks, Alaska, 1, 457- 462, 2008.

21 Gagnon, R.M., and Ferland, M.-: Climat du Québec septentrional. Québec, Service de la  
22 météorologie. Ministère des richesses naturelles, 107, 1967.

23 GAMMA Remote Sensing AG: Differential Interferometry and Geocoding Software –  
24 DIFF&GEO. Vers.1.2. Gümligen, 2008.

25 Ge, L., Zhan, K., Alex, Ng., Dong, Y., Hsing-Chung, C., and Rizos, C.: Preliminary Results  
26 of Satellite Radar Differential Interferometry for the Co-seismic Deformation of the 12  
27 May 2008 Ms8.0 Wenchuan Earthquake, Lect Notes Comput Sc, 14, 12- 19, 2008.

28 Goldstein, R. M., Engelhard, R., Kamb, B., and Frohlich, R.: Satellite radar interferometry for  
29 monitoring ice sheet motion: Application to an Antarctic ice stream, Science, 262, 1525 –  
30 1530, 1993.

- 1 Gurney, SD.: Aspects of the genesis, geomorphology and terminology of palsas: perennial  
2 cryogenic mounds, *Prog Phys Geog*, 29: 139-155, 2001.
- 3 Hanssen, R. F.: *Radar Interferometry. Data Interpolation and Error Analysis*. Kluwer  
4 Academic Pub, New York, 2001.
- 5 Hofmann-Wellenhof, B., Lichtenegger, H., and Wasle, E.: *GNSS – Global Navigation*  
6 *Satellite Systems*. Springer, Wien, New York, 2008.
- 7 Kaufmann, V.: Deformation analysis of the Doesen rock glacier (Austria), in: Proceedings 7  
8 th International Conference on Permafrost, Lewkowitz AG, Allard M (eds). Centre  
9 d'études Nordiques, Université Laval: Quebec Nordicana 57, 23–27 June 1998, 551-556,  
10 1998.
- 11 Kranck, E. H.: On the geology of the east coast of Hudson Bay and James Bay, observations  
12 during a research journey in summer 1947, *Acta Geogr.*,11, 1-71, 1951.
- 13 Laberge M.J., and Payette S.: Long-Term Monitoring of Permafrost Changes in a Palsa  
14 Peatland in Northern Quebec, Canada: 1983-1993. *Arctic and Alpine Research*, 27,  
15 167-171, 1995.
- 16 Lajeunesse, P., and Allard, M. The Nastapoka drift belt, eastern Hudson Bay: implications of  
17 a stillstand of the Quebec-Labrador ice margin in the Tyrrel Sea at 8 ka BP, *Can J Earth*  
18 *Sci*, 40, 65-76, 2003.
- 19 Larsen, Y., Lauknes, T.R., and Christiansen, H.H.: Seasonal Periglacial Activity in Permafrost  
20 Landscapes Measured with High-Resolution InSAR Time Series. 4. TerraSAR- X  
21 Science Team Meeting, 14 - 16. February, 2011, Oberpfaffenhofen, Deutschland, 2011.
- 22 Larsen, Y., Lauknes, T. R., Malnes, E., and Christiansen, H. H.: High-resolution InSAR  
23 analysis of Radarsat-2 Ultra-Fine mode and TerraSAR-X data for measuring fine-scale  
24 landscape changes due to permafrost activity, 6th International Workshop on SAR  
25 Interferometry: Advances in the Science and Applications of SAR Interferometry  
26 (FRINGE 2009), ESA ESRIN, Frascati, Italy, 30.November – 4. December, 2009, 2009.
- 27 Lauknes, T. R., Larsen, Y., Malnes, E., and Christiansen, H. H. : Permafrost monitoring  
28 using SAR and ground based techniques in Svalbard, Third European Conference on  
29 Permafrost (EUCOP III), Longyearbyen, Svalbard, Norway, 13.- 17. June 2010, 2010a.

- 1 | Lauknes, T. R., Larsen, Y., Malnes, E., and Christiansen, H. H.: Monitoring of periglacial  
2 | landform changes in permafrost landscape using radar satellite time series, ESA Living  
3 | Planet Symposium 2010, Bergen, Norway, 28. June – 2. July 2010, 2010b.
- 4 | Little, J.D.: Frost heave and thaw settlement in Tundra Environments: Applications of  
5 | Differential Global Positioning System Technology. Ph.D. thesis. Faculty of the  
6 | University of Delaware, Newark, USA, 160 pp., 2006.
- 7 | Little, J.D., Sandall, H., Walegur, M.T., and Nelson, F.E.: Application of differential global  
8 | positioning systems to monitor frost heave and thaw settlement in tundra environments.  
9 | Permafrost Periglac, 14, 349-357, 2003.
- 10 | Liu, L., Zhang, T., and Wahr, J.: InSAR measurements of surface deformation over  
11 | permafrost on the North Slope of Alaska, J Geophys Res, 115, F03023,  
12 | doi:10.1029/2009JF001547, 2010.
- 13 | Liu, L., Zhang, T., Shaefer, K., and Wahr, J.: InSAR Observations Revealed Surface  
14 | Subsidence over permafrost in Northern Alaska, Alaska Satellite Facility, News and  
15 | Notes, Fairbanks, Alaska, USA, 7, 2011.
- 16 | Mackay, J.R.: Seismic shot holes and ground temperatures, Mackenzie Delta area, Northwest  
17 | Territories. Geological Survey of Canada Paper, Ottawa, Canada, Part A, 74, 389-390,  
18 | 1974.
- 19 | May I.: Using in-field and remote sensing data to monitor permafrost dynamics in Northern  
20 | Québec. Ph.D. thesis, Ludwig-Maximilians University of Munich, Germany, 181 pp.,  
21 | 2011.
- 22 | Nelson, F., Anisimov, O., and Shiklomanov, N.: Subsidence risk from thawing permafrost,  
23 | Nature, 410, 889-890, 2001.
- 24 | Nelson, F.E., Brigham, L., Hinkel, K.M., Romanovsky, V.E., Smith, O., Tucker, W., and  
25 | Vinson, T.: Climate Change, Permafrost and Impacts on Civil Infrastructure. Special  
26 | Report 01-03, Permafrost Task Force, U.S. Arctic Research Commission, Arlington, VA.  
27 | 72 pp, 2003.
- 28 | Nelson, F.E., Shiklomanov, N.I., Mueller, G.R., Hinkel, K.M., Walker, D.A., and Bockheim,  
29 | J.G.: Estimating active-layer thickness over a large region: Kuparuk River basin, Alaska,  
30 | U.S.A.. Arctic Alpine Res, 29, 367 -378, 1997.

- 1 Phillips, D.W.: Climatic atlas Canada: a series of maps portraying Canada's climate, Ottawa,  
2 Canada. In Gouvernement du Canada (Ed.) (1984). Climatic atlas Canada: a series of  
3 maps portraying Canada's climate, Ottawa, Canada, 1984.
- 4 Pissart, A.: Palsas, lithalsas and remnants of these periglacial mound. A progress report, Prog  
5 Phys Geog, 26, 605 – 621, 2002.
- 6 Pissart, A.: Remnants of lithalsas of the Hautes Fagnes, Belgium: a summary of present-day  
7 knowledge, Permafrost Periglac, 11, 327-355, 2000.
- 8 Romanovsky, V.E., and Osterkamp, T.E.: Interannual variations of thermal regime of active  
9 layer and near-surface permafrost in northern Alaska, Permafrost Periglac, 6, 313-335,  
10 1995.
- 11 Rowland, J.C., Jones, C.E., Altmann, G., Bryan, R., Crosby, B.T., Geernaert G.L., Hinzmann,  
12 L.D., Kane, D.L., Lawrence, D.M., Mancino, A., Marsh, P., McNamara, J.P.,  
13 Romanovsky, V.E., Toniolo, H., Travis, B.J., Trochim, E., and Wilson, C.J.: Arctic  
14 Landscapes in Transition: Responses to Thawing Permafrost. EOS, Transactions,  
15 American Geophysical Union, 91, 229 – 236, 2010.
- 16 Seppälä, M.: Palsas and related forms, in: Advances in periglacial geomorphology, Clark,  
17 M.J. (Ed.), Chichester: Wiley Chapter 11, 247-278, 1988.
- 18 Shiklomanov, N.I., Streletskiy, D.A., Little, J.D., and Nelson, F.E.: Isotropic thaw subsidence  
19 in undisturbed permafrost landscapes. Geophys Res Lett, 40, 24, 6356 – 6361, 2013.
- 20 Short, N., Brisco, B., Couture, N., Pollard, W., Murnaghan, K., and Budkewitsch., P.: A  
21 comparison of TerraSAR-X, RADARSAT-2 and ALOS-PALSAR interferometry for  
22 monitoring permafrost environments, case study from Herschel Island, Canada, Remote  
23 Sens Environ, 15, 3491-3506, 2011.
- 24 Short N., LeBlanc A.-M, Sladen W., Oldenborger G., Mathon-Dufour, V., and Brisco, B.:  
25 RADARSAT-2 D-InSAR for ground displacement in permafrost terrain, validation from  
26 Iqaluit Airport, Baffin Island, Canada, Remote Sens Environ, 141:40-51, 2014.
- 27 Skaven-Haug, S.: Protection against frost heaving on Norwegian railways, Geotechnique, 9,  
28 87-106, 1959.
- 29 Smith, S.L., Mac Donald, G.M., Velichko, A.A, Beilman, D.W., Borisova, O.K., Frey, K.E.,  
30 Kremenetski, K.V., and Sheng; L., Y.: Siberian Peatlands a Net Carbon Sink and Global  
31 Methane Source Since the Early Holocene, Science, 303, 353-356, 2004.

- 1 Smith, S.L., Romanosky, V.E., Lewkowicz, A.G., Bum, C.R., Allard, M., Clow, G.D.,  
2 Yosikawa, K., and Throop, J.: Thermal State of Permafrost in North America: A  
3 Contribution to the International Polar Year, *Permafrost Periglac*, 21, 117-135, 2010.
- 4 Spannraft, K.: Using X-band Differential SAR Interferometry to monitor seasonal surface  
5 deformation in a permafrost landscape in Nunavik, Québec. Diploma thesis, Ludwig-  
6 Maximilians University Munich, Germany, 149 pp., 2010.
- 7 Strozzi T., Grosse, G., and Streletsij, D.: SAR Interferometry for surface deformation  
8 monitoring in Permafrost Areas in Alaska, *Proc. Earth Observation and Cryosphere  
9 Science Conf.*, Frascati, Italy, 13-16 November 2012, 2012.
- 10 Sushama, L., Laprise, R., and Allard, M.: Modeled current and future soil thermal regime for  
11 northeast Canada, *J Geophys Res*, 111, D18111, doi:10.1029/2005JD007027, 2006.
- 12 Tait, M., and Moorman, B.: A Feasibility Study into monitoring deformation in the Niglintgak  
13 regions of the Mackenzie Delta, in: *Proceedings, 11th FIG Symposium on Deformation  
14 Measurements: Santorini, Greece, 25–28 May, 2003*, E8, 2003.
- 15 Tait, M., Sheng, L., and Cannon, E.: The feasibility of replacing precise levelling with GPS  
16 for permafrost deformation monitoring, in: *Proceedings of the FIG 3rd International  
17 Conference on Engineering Surveying, Bratislava, Slovakia, 1 November, 2004*.
- 18 Tait, M., Moorman, B., and Sheng, L.: The long-term stability of survey monuments in  
19 permafrost, *Eng Geol*, 79, 61-79, 2005.
- 20 Theakstone, W.H., Jacobsen, F.M., and Knudsen, N.T.: Changes of snow cover thickness  
21 measured by conventional mass balance methods and by Global Positioning System  
22 surveying. *Geografiska Annaler* 81A, 767-77, 1999.
- 23 Trimble: [www.trimble.com/gps/dgps-advanced2.shtml](http://www.trimble.com/gps/dgps-advanced2.shtml), 2010, last access: 11.November 2013.
- 24 UNVACO:[http://www.unavco.org/projects/project-support/polar/base\\_stations\\_and\\_survey\\_  
25 systems/base\\_stations\\_and\\_survey\\_systems.html](http://www.unavco.org/projects/project-support/polar/base_stations_and_survey_systems/base_stations_and_survey_systems.html). 2014, last access: 20. August 2014.
- 26 [Wegmüller, U., and Werner, C.: Land applications using ERS-1/2 tandem data. Proc. of the  
27 Fringe 96 Workshop: ERS SAR Interferometry, Zurich, 30 September – 2 October 1996,  
28 ESA SP-406, 97–112, 1996.](#)
- 29 Wirz, V., Geertsema, M., Gruber, S., and Purves R.S.: Temporal variability of diverse  
30 mountain permafrost slope movements derived from multi-year daily GPS data,  
31 Matternal, Switzerland. *Landslides*, 1-17, doi: 10.1007/s10346-014-0544-3, 2015.

1 Yen, J.-Y., Chen, K.-S. Chang, C.-P., and Boerner, W. –M.: Evaluation of earthquake  
 2 potential and surface deformation by differential interferometry. Remote Sens Environ,  
 3 112, 782-795, 2008.

4 Zebker, H.A., and Villasenor, J.: Decorrelation in interferometric radar echoes, IEEE Trans.  
 5 Geo. Rem. Sensing, Vol 30, no. 5, 950-959, September, 1992.

6 Zoltai, S.C., and Tarnocai, C. : Perennially frozen peatlands in the western Arctic and  
 7 Subarctic of Canada, Can J Earth Sci, 12, 28–43, 1975.

8 Zuidhoff, F. S.: Recent decay of a single palsa in relation to weather conditions between 1996  
 9 and 2000 in Laivadalen, northern Sweden, Geogr. Ann. A., 84, 103-111, 2002.

10 Zuidhoff, F.S., and Kolstrup, E.: Palsa development and associated vegetation in northern  
 11 Sweden, Arct Antarct Alp Res, 37, 49-60, 2005. SHAPE , 2005.

12 ~~Table 1. Acquisition dates for the d-GPS and TerraSAR-X data and details of the useable~~  
 13 ~~differential interferograms considered in this study~~

14  
 15  
 16  
 17

18 Table 1. Acquisition dates for ~~the~~d-GPS and TerraSAR-X data and details of the useable  
 19 differential interferograms considered in this study.

20

Year	D-GPS acquisition dates	TerraSAR-X acquisition dates	Detailed dates of useable interferograms		
			Dates	Temporal baseline [d] *	Perpendicular baseline [m] **
2009	20.04	07.05	07.05 / 14.08	99	125.36
	14.08	14.08			
		25.08	14.08 / 25.08	11	-66.79
		27.09			
		30.10	14.08 / 30.10	55	12.78

<b>2010</b>	25.03	22.03			
	08.05	05.05	05.05 / 12.08	99	0.43
	12.08	12.08			
		23.08	12.08 / 23.08	11	-159.00
	27.10	28.10	12.08 / 28.10	77	-195.41
<b>2011</b>	09.04				

\*time delay between the acquisitions

\*\*separation in meters between two antenna positions

1

	<u>Lithalsa R</u>	<u>Lithalsa M</u>	<u>Lithalsa I</u>
<u>Diameter [m]</u>	<u>40</u>	<u>40</u>	<u>40</u>
<u>Soil</u>	<u>Aeolian sediments (Sand, silt, gravel)</u>	<u>Marine and littoral sediments (sand)</u>	<u>Aeolian sediments (Sand, silt, gravel)</u>
<u>Vegetation</u>	<u>Bare ground, lichens, prostrate shrubs</u>	<u>Bare ground, lichens, prostrate shrubs</u>	<u>Bare ground, lichens, prostrate shrubs</u>
<u>Ponds</u>	<u>Ca. 220 m<sup>2</sup> at east slope</u>	<u>Ca. 65 m<sup>2</sup> at north slope</u>	=
<u>Degradation status</u>	<u>Advanced cracks visible</u>	<u>Cracks visible</u>	=

2 Table 2. Characteristics of the three lithalsas

3

4 Table 32. Characteristics of the TerraSAR-X sensor and the acquisition mode used for this  
5 study (based on CAF, 2009)

<b>Spatial resolution:</b>		<b>Acquisition mode:</b>	
Swath width	~ 15 km	Sensor mode	Stripmap

Slant range resolution	1.2 km	Polarization mode	Dual (VV)*
Ground range resolution - Incidence angle: 40°	1.8 m	Pass & look direction	Ascending/ Right
		Product type	SSC**
Range pixel spacing	0.9 m	Local acquisition time	6.46 pm
Azimuth pixel spacing	2.5 m	Processing level	L1B
*VV: vertical/ vertical                      **SSC: Single Look Slant Range Complex			

1

2

1 | Table 43. Average coherence over the three lithalsas for the six interferograms

	2009			2010		
	14.08_07.05	14.08_25.08	14.08_30.10	12.08_05.05	12.08_23.08	12.08_28.10
<b>Lithalsa R</b>	<b>0.17</b>	<b>0.18</b>	<b>0.24</b>	<b>0.10</b>	<b>0.20</b>	<b>0.215</b>
<b>Lithalsa M</b>	<b>0.14</b>	<b>0.20</b>	<b>0.14</b>	<b>0.13</b>	<b>0.19</b>	<b>0.15</b>
<b>Lithalsa I</b>	<b>0.12</b>	<b>0.34</b>	<b>0.154</b>	<b>0.13</b>	<b>0.46</b>	<b>0.10</b>

2

1

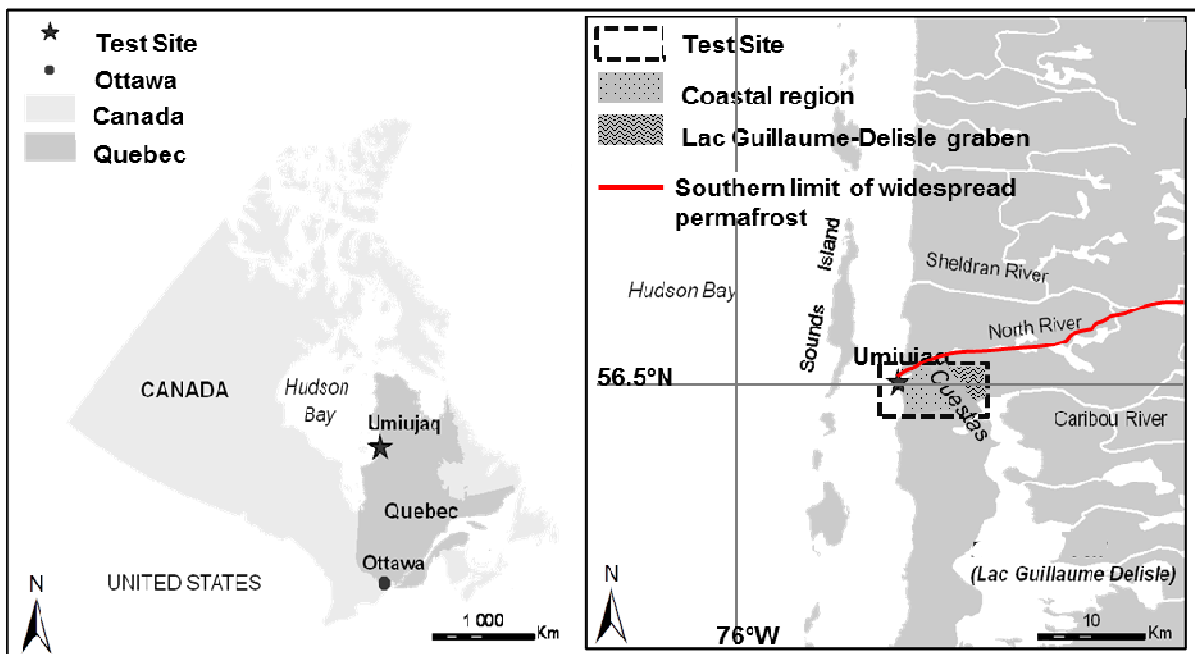


2

Figure 1A. One exemplary A typical lithalsa within the study area near Umiujaq (northern Quebec), with a diameter of 20 m. The picture has been Photo taken in April 2009, to the east of the Cuestas (56°33'N 76°28' W)

Figure 1B. Thermokarst pond and eroding slope on L of lithalsa R.

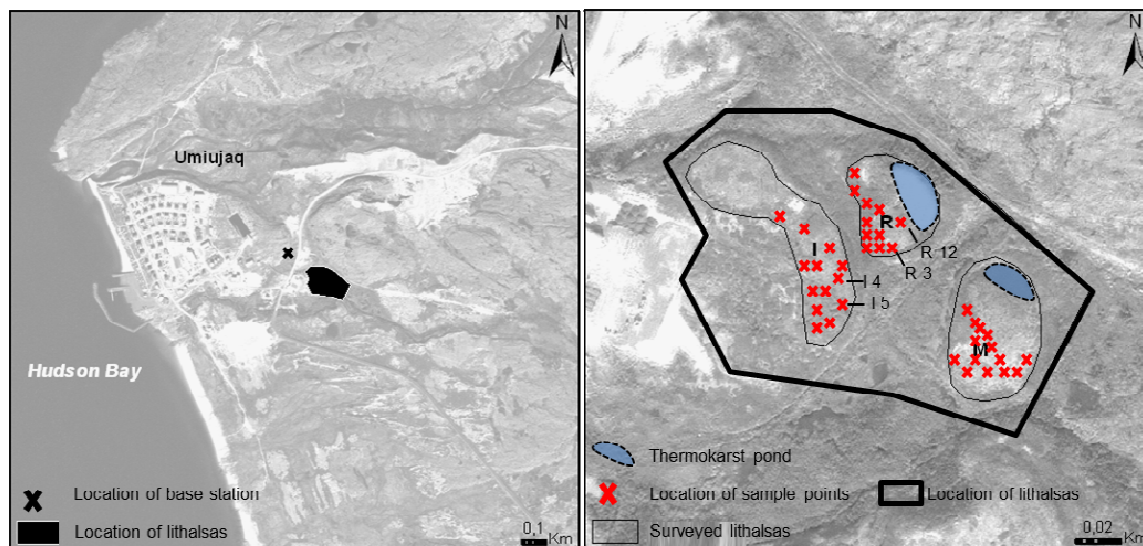
Figure 1C. Cracks up to 0.5 m deep at on slope of L lithalsa R. They are up to 0.5 m high.



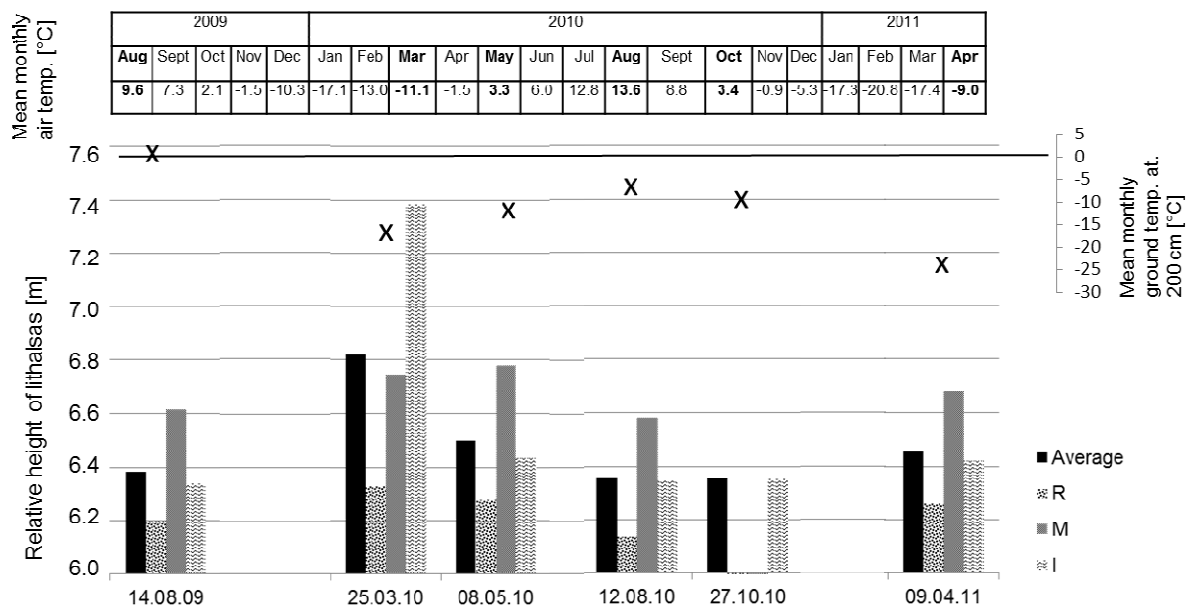
3

4 Figure 2. Location of the study area in the vicinity of Umiujaq, northern Quebec, Canada  
 5 (left), and the distribution of the two main types of landscape types (right): the coastal region  
 6 to the west of the Cuestas and the Lac Guillaume-Delisle graben to the east of the Cuestas.

1 The approximate boundary between widespread discontinuous permafrost to the north and  
 2 scattered-sporadic permafrost to the south (based on Allard and Séguin, 1987) is shown in red.



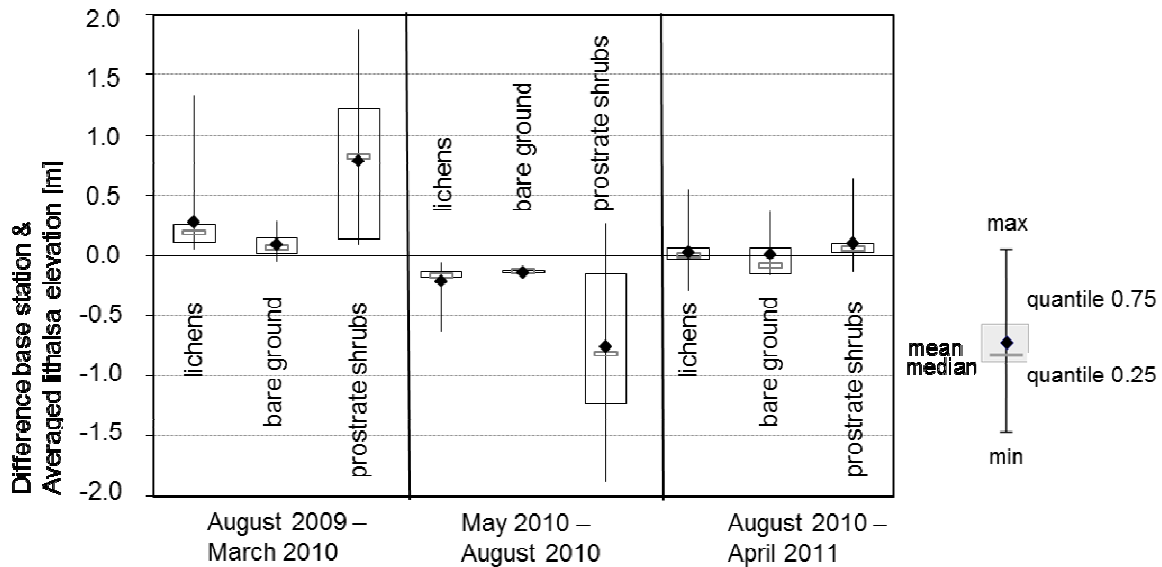
3  
 4 Figure 3. Left: location of the surveyed lithalsas and the base station, south-east of Umiujaq  
 5 (background: GeoEye image from 25.09. 2009). Right: enlargement showing the three  
 6 lithalsas (I, R and M) and the locations of the individual measurements points. The identified  
 7 measurement points (R3, R12, I4, I5) are specifically discussed in Section 4.



8  
 9 Figure 4. Heights of the three lithalsas (grey bars) and their average (black  
 10 bars), relative to the base station, on the 6 measuring dates spread over a 20 month period.  
 11 The heights represent the average of heights from all measurement points within each  
 12 individual lithalsa. The accuracy of the records amounts to several centimeters The records are

1 accurate to within a few centimeters. The lithalsas were not covered by snow during the  
 2 measurements. The temperatures at the top are the mean monthly air temperatures of the  
 3 specific ~~year provided~~ year provided (CEN, 2013). Temperatures written in bold are for the  
 4 month with d-GPS measurements.  
 5 by Environment Canada (2004).

6



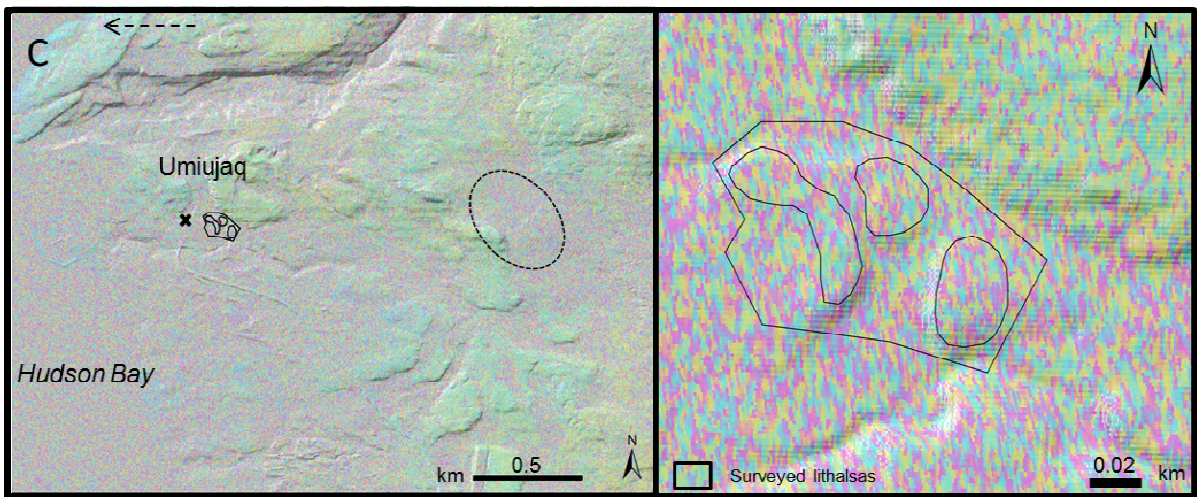
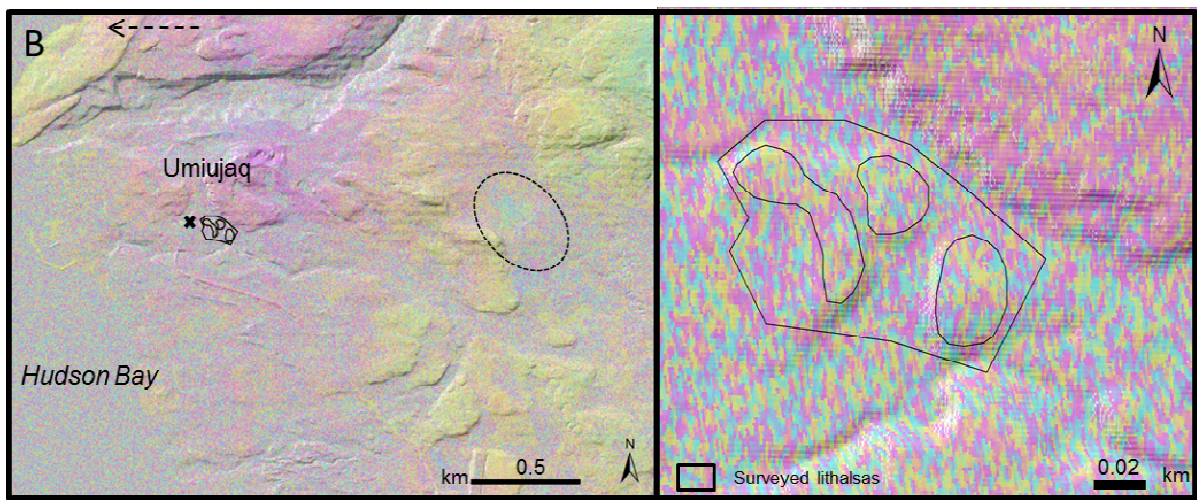
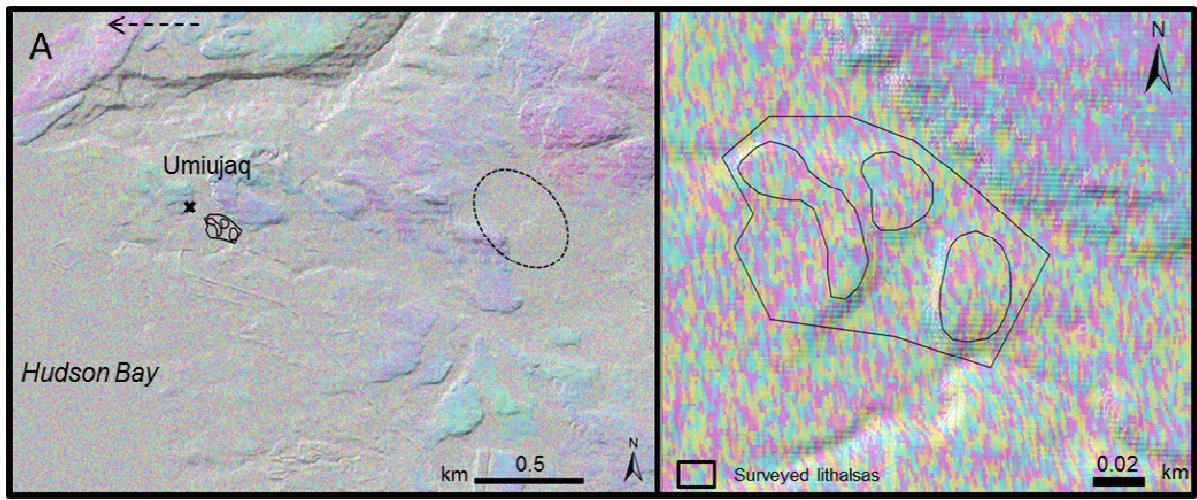
7

8 Figure 5. Box plots of surface cover and elevation changes for the three lithalsas, measured  
 9 between August 2009 and March 2010, between May 2010 and August 2010, and between  
 10 August 2010 and April 2011, based on all 39 measurement points on the three lithalsas.

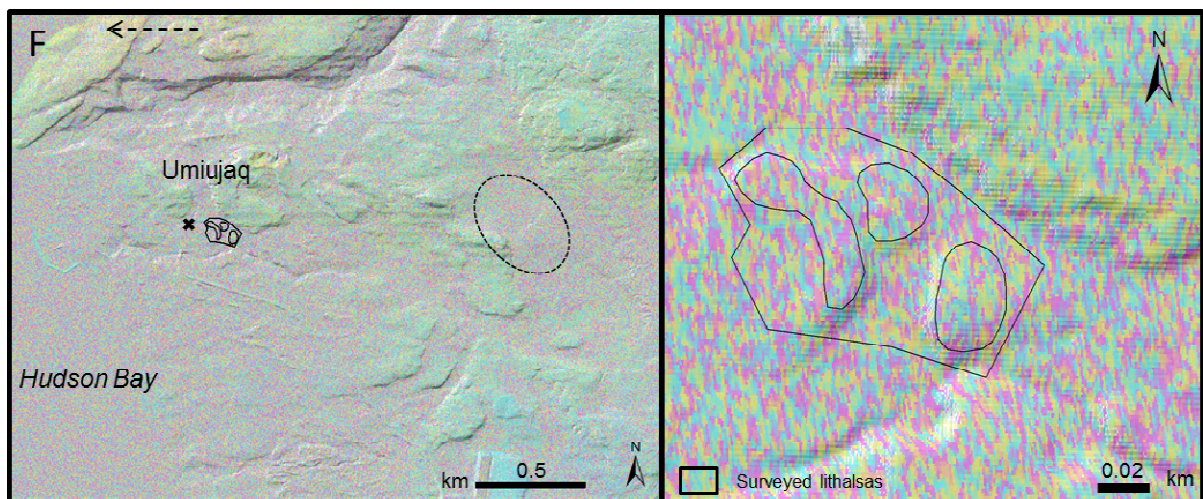
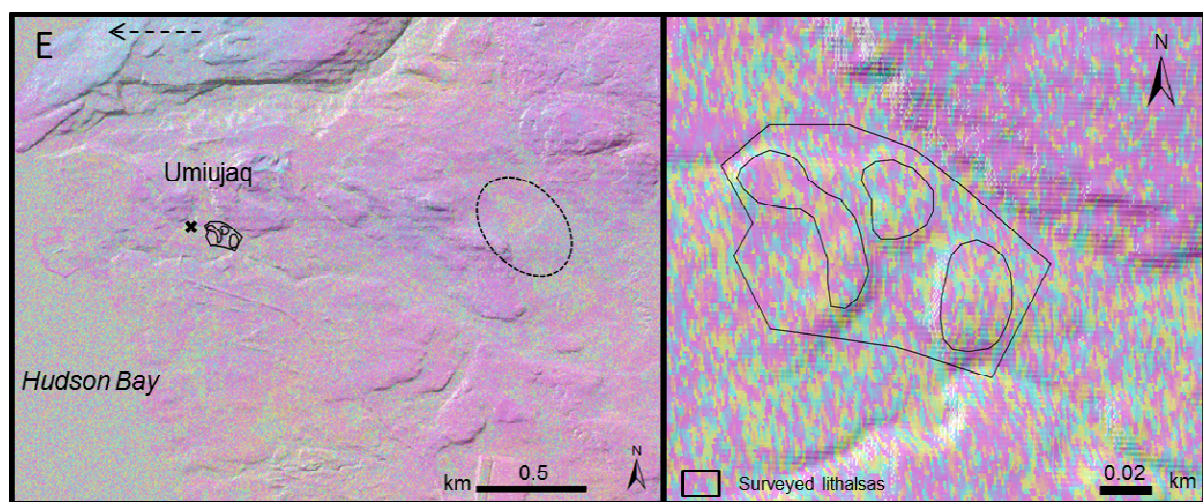
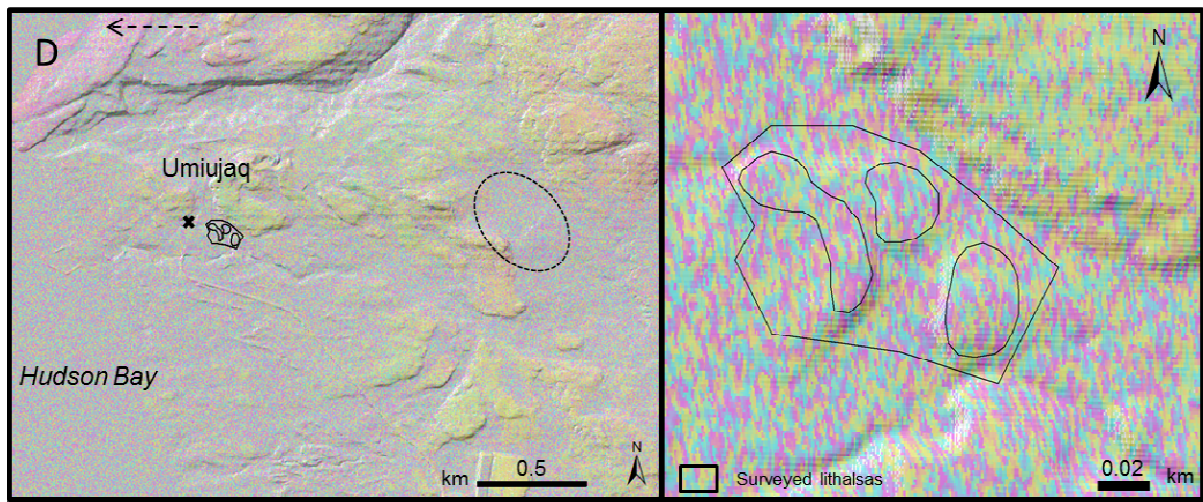


1  
2  
3  
4  
5

Figure 6. Photo taken in April 2010 showing sparse snow cover on the lithalsas (Lithalsa M in this case) during the field visits.



1



1  
 2 | Figure 67a. The six interferograms (A: 14.08.09-07.05.09, B: 14.08.09-25.08.09, C: 14.08.09-  
 3 | 30.10.09, D: 12.08.10-05.05.10, E: 12.08.10-23.08.10, and F: 12.08.10-28.10.10). Left: broad

1 area around Umiujaq, northern Quebec, Canada. The dashed arrow to the north of Umiujaq  
 2 indicates the fringes of slow movements; the dotted circles indicates the area of signals to the  
 3 east of the lithalsas. Right: ~~the~~ area-of covering the three lithalsas of interest; the amount of  
 4 movement exceeds the amount that can be quantified with TerraSAR-X data.

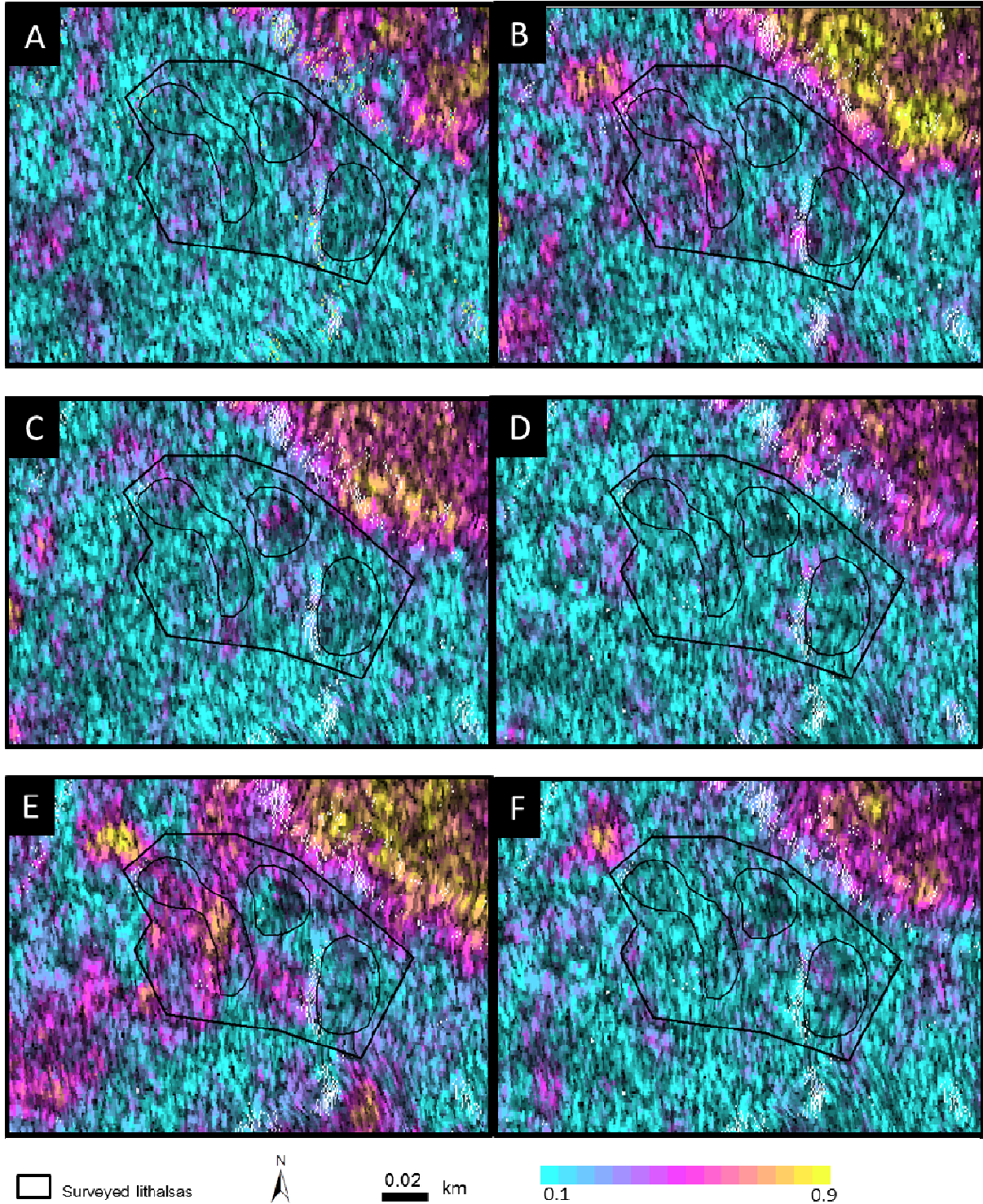


Figure 67b. The coherence values of the six interferograms in the area of the three lithalsas of interest, near Umiujaq, northern Quebec, Canada (A: 14.08.09-07.05.09, B: 14.08.09-

- 1 | 25.08.09, C: 14.08.09-30.10.09, D: 12.08.10-05.05.10, E: 12.08.10-23.08.10, and F: 12.08.10-
- 2 | 28.10.10)